# Study of the horn effect on curved surfaces

Stefan Gombots[1], Manfred Kaltenbacher[2]

[1] *Institute of Mechanics and Mechatronics, 1060 Vienna, Austria, Email: stefan.gombots@tuwien.ac.at*

[2] *Institute of Mechanics and Mechatronics, 1060 Vienna, Austria, Email: manfred.kaltenbacher@tuwien.ac.at*

## Introduction

The dominant noise component of road traffic is generated by the tire rolling on the road surface. The tire-road noise is influenced by the roughness of the surface and the tread pattern of the tire. In this context, the horn effect is known as an amplification mechanism of the tire-road noise radiation. The horn-shaped geometry between the tire and the road surface leads to an amplification of the sound pressure level. Usually, the tire is running on a flat road surface. In some cases, e. g. test stands, the tire will run on a curved surface, where the curvature can be convex or concave. The influence of the curvature will be investigated by using the finite element method (FEM) for solving the radiation problem.

## Theory

The tire-road noise is an important component related to traffic noise. Measurements were taken in Europe with a trailer applying the close-proximity method (CPX) [1]. Here, two microphones are mounted near the sidewall of the tire in a trailer lined with sound absorbing material. In Austria, additionally the RVS 11.066 [2] is used, having also two microphones and a trailer in usage. In the US the on-board sound intensity (OBSI) method [3] is used, where two intensity probes are placed alongside the leading and traling edge of the tire. Different from CPX and RVS, OBSI doesn't use a trailer. The intensity probes are mounted directly on the vehicle. During the measurements ambient conditions like vehicle speed, temperature, wind speed, etc. have also to be recorded. The tire-road noise can also by measured using test stands, obtaining some advantages compared to the outdoor measurements. The weather-dependence can be neglected and additional measurement technology can be used. On the other hand, one have to deal with some restrictions, e. g. self-noise of the test stand, sound reflections, a realistic road surface and tire-road contact, etc. Outer and inner drum test stands are often used for measurements. Here, the tire is rolling on a concave respectively convex surface. Due to this fact the contact patch will be different than a tire on a flat surface. Here, the influence of such a curvature on the horn effect is studied.

## Horn effect

The geometry between tire and road surface is shaped like an exponentially horn (see Fig. 1). Through the impedance jump due to the change of the geometry the radiated sound will be amplified. The amplification of the sound pressure level (SPL) lies between 7 and 20 dB [4],

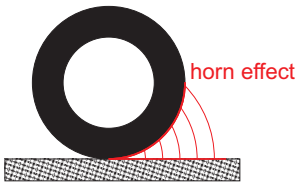


**Figure 1:** Geometry between tire and a flat road surface. The horn effect leads to an amplification of the sound pressure level.

depending on the frequency and the observation point. The so called horn effect is highly developed at wave lengths, which are approximately equal to the tire radius [5]. The amplification caused by the horn effect depends also on the road surface and the geometry of the tire. On sound absorbing road surfaces the effect is less pronounced. Furthermore, the tire diameter and the wideness of the tire influence the effect. Large and wide tires leads to high sound amplification [6].

## Simulations

In the following, the influence of a concave curvature on the horn effect is investigated. This situation is present, e. g. on an inner drum test stand. In Fig. 2 the cross section of the simulation model is depicted.

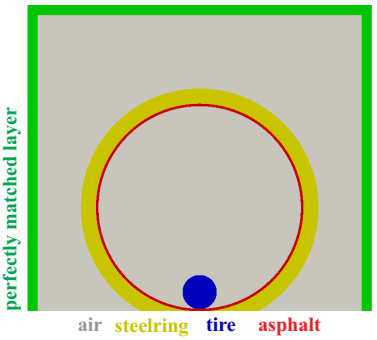


**Figure 2:** Cross section of the simulation model.

The tire and the steel ring were modelled acoustically hard. In the simulation a slick 225/60 R16 tire was used. Hence, the tread pattern was neglected. To achieve free field conditions a perfectly matched layer (PML) was used. For the study different diameters of the ring were considered (see Fig. 3(c)-(d)). Furthermore, two different types of asphalt have been used in the simulations. To quantify the effect of different curvatures on the horn effect two reference setups were used. Setup 1 in which the tire is omitted (Fig. 3(a)) and setup

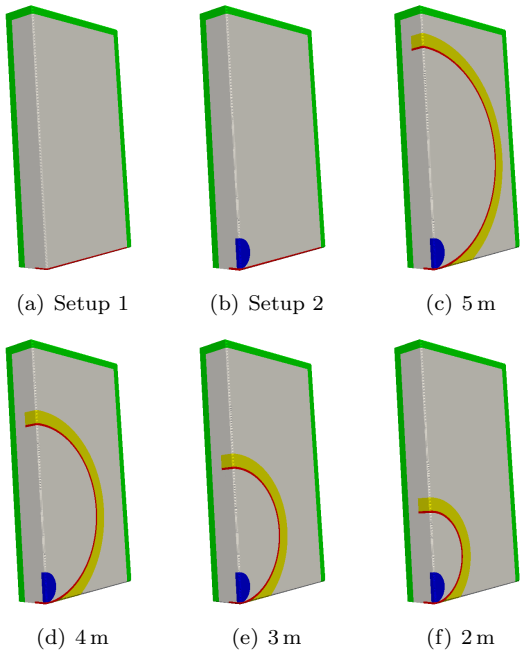

(a) Setup 1 (b) Setup 2 (c) 5 m

(d) 4 m (e) 3 m (f) 2 m

**Figure 3:** The two reference setups and the models with different diameters of the steelring.

2 where the tire is present in the simulation domain (Fig. 3(b)). For purposes of comparison, the size of all models (6.4 m × 2.0 m × 5.8 m) and the position of the sound excitation were the same in all simulations. The sound excitation was realized by 5 nodes on the trailing edge between tire and road surface in the center of the horn shaped geometry. The simulations were done with the FEM-code CFS++ [7]. In the simulations frequencies between 500 Hz and 1500 Hz were considered, since in this frequency band tire-road noise is dominant [4].

## Asphalt modeling

As mentioned earlier, two different asphalt types were considered. The two types in the simulations are AC8 (asphalt concrete) and SMA/LA8 (low-noise stone mastic asphalt). As one can see in Fig. 4 the absorption coefficient of AC8 is quite small, and therefore this type was modeled acoustically hard. One the other hand, the SMA/LA8 leads to some absorption. The SMA/LA8 asphalt is like a porous absorber. The porous asphalt can be considered as a layer of an equivalent complex fluid having a frequency-dependent effective density $\tilde{\rho}_{\text{eff}}$ and bulk modulus $\tilde{K}_{\text{eff}}$. To get the parameters the Zwikker and Kosten model was used [9]. For the effective density and the bulk modules one obtains

$$\tilde{\rho}_{\text{eff}}(\omega) = \rho_0 \left[ 1 + \frac{1}{\sqrt{3^2 + \frac{4\omega\rho_0}{\sigma\phi}}} - j\frac{\sigma\phi}{\omega\rho_0}\sqrt{1 + \frac{\rho_0\omega}{4\sigma\phi}} \right] \quad (1)$$

$$\tilde{K}_{\text{eff}}(\omega) = \frac{\gamma p_0}{\gamma - (\gamma - 1)\left[1 - \frac{\text{Nu}}{j8\omega\rho_0\text{Pr}/\sigma\phi + \text{Nu}}\right]}. \quad (2)$$

The porosity $\phi$ and air flow resistivity $\sigma$ was chosen according to measurement results [8]. The parameters for modeling the SMA/LA8 asphalt are depicted in Tab. 1.

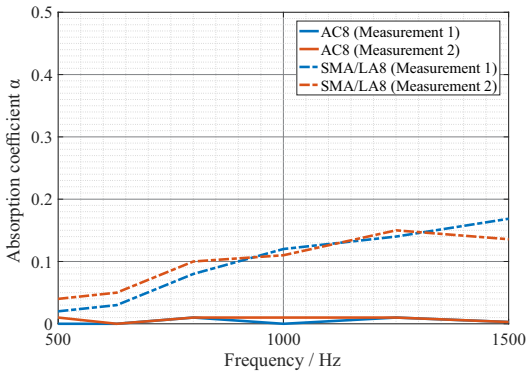


**Figure 4:** Measurement results of the absorption coefficient of AC8 and SMA/LA8 asphalt [8].

**Table 1:** Model parameters.

| Parameter | Unit | Value |
|---|---|---|
| Prandtl number Pr | - | 0.71 |
| Nusselt number Nu | - | 3.10 |
| Static pressure $p_0$ | Pa | $1.013 \cdot 10^5$ |
| Air density $\rho_0$ | $\text{kg m}^{-3}$ | 1.213 |
| Ratio of specific heat $\gamma$ | - | 1.4 |
| Angular frequency $\omega$ | $\text{s}^{-1}$ | $2\pi\,[500 \ldots 1500]$ |
| Air flow resisivity $\sigma$ | $\text{Pa s m}^{-2}$ | 3000 |
| Porosity $\phi$ | % | 10 |

To validate the model parameters of the asphalt the absorption coefficient was determined by the transfer-function method (2p-method) [10]. In Fig. 5 the simulation result is displayed, which shows a good agreement with the measurement results.

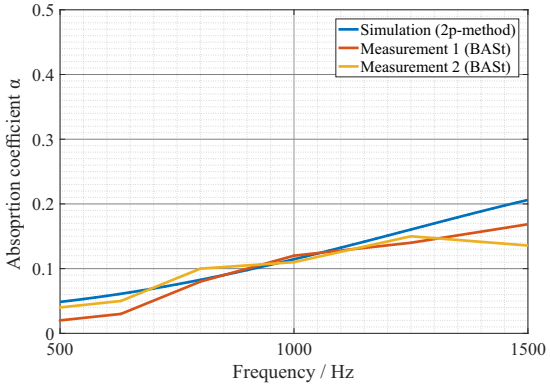


**Figure 5:** Validation result obtained by the transfer function method. Comparison with measurement results done at BASt (Bundesanstalt für Straßenwesen).

## Evaluation

To compare the different models (Fig. 3) the sound pressure level difference ΔSPL and the sound power level difference ΔSPW were used. The ΔSPL is obtained by

$$\Delta\text{SPL} = \text{SPL}(\boldsymbol{x}) - \text{SPL}_{\text{ref}}(\boldsymbol{x}) = 20\log_{10}\frac{p(\boldsymbol{x})}{p_{\text{ref}}(\boldsymbol{x})}, \quad (3)$$

where the $\text{SPL}(\boldsymbol{x})$ denotes the sound pressure level and $p(\boldsymbol{x})$ the sound pressure at a monitoring point $\boldsymbol{x}$. For the

sound power level difference one has

$$\Delta\mathrm{SPW} = \mathrm{SPW} - \mathrm{SPW}_{\mathrm{ref}} = 10\log_{10}\frac{P_{\mathrm{a}}}{P_{\mathrm{a,ref}}}, \qquad (4)$$

with SPW as the sound power level and $P_{\mathrm{a}}$ the sound power. For the calculation of the sound power the area at the interface to the PML was used. The subscript ref indicates that the value at the reference setup is used.
First, setup 1 (see Fig. 3(a)) and setup 2 (see Fig. 3(b)) were compared to determine the horn effect on a flat road surface. The used monitoring points are displayed in Fig. 6. One of the monitoring points (RVS-1) coincides with a measurement position in the RVS 11.066.

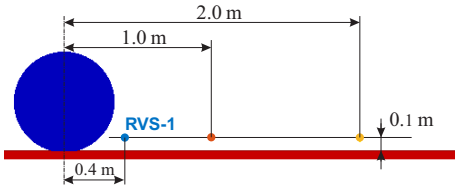


**Figure 6:** Three monitoring points for the determination of the horn effect on a flat road surface.

The reference for the determination of the pressure in the presence of a tire is setup 1, there the tire was omitted. The result of the ΔSPL is given in Fig. 7 and for ΔSPW in Fig. 8.

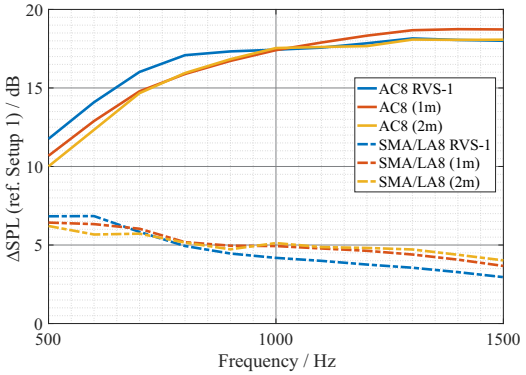


**Figure 7:** ΔSPL on AC8 and SMA/LA8 at varying monitoring positions.

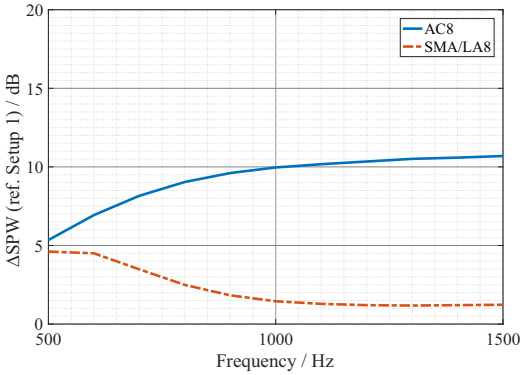


**Figure 8:** ΔSPW on the two different asphalt types.

One can clearly see the effect of a sound absorbing road surface. The amplification of the SPL on the SMA/LA8 is quite lower than on the AC8. Moreover, at the low-noise asphalt the amplification is almost the same in the considered frequency range. Furthermore, the monitoring point RVS-1 shows different behavior than the monitoring points in a larger distance.
Next, the different diameters of the ring will be compared. For this reason, setup 2 was chosen as the reference setup to show the influence of the curvature on the SPW and SPL. To determine the ΔSPL the sound pressure at the RVS-1 position was used. At the smallest ring diameter the deviations are largest. On the non-absorbing asphalt AC8 the deviation is slightly higher. In addition, the ΔSPL over frequency shows a non-monotonically behavior, which is caused by standing waves in the ring. Thereby, the standing wave field on the reflecting asphalt AC8 is more remarkable. Furthermore, at a higher ring diameter the deviations becomes less. The simulation results are depicted in Fig. 9.

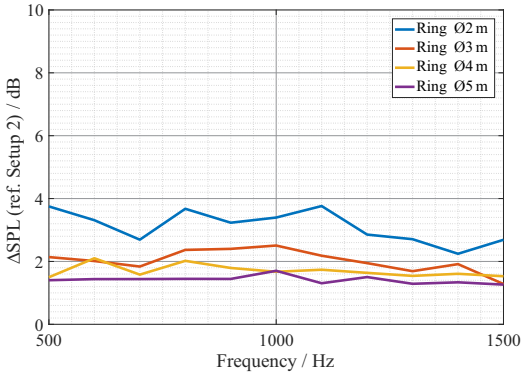


(a)

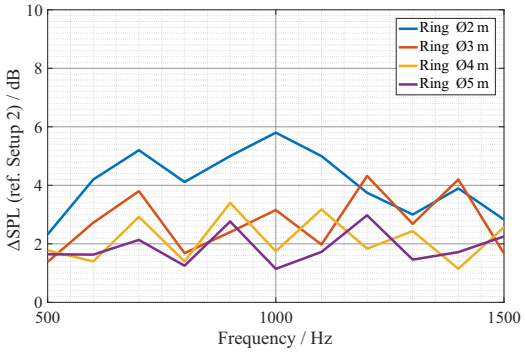


(b)

**Figure 9:** (a) ΔSPL on various ring diameters on SMA/LA8 (b) ΔSPL on various ring diameters on AC8.

The results for the sound power are showing different behavior. In the case of the absorbing asphalt SMA/LA8, the ΔSPW becomes negative at higher frequencies, i. e. the sound power decreases. On the AC8 the behavior is the same like in the sound pressure results.
For all simulations on the different ring diameters, whether for ΔSPL or ΔSPW the same conclusion holds;

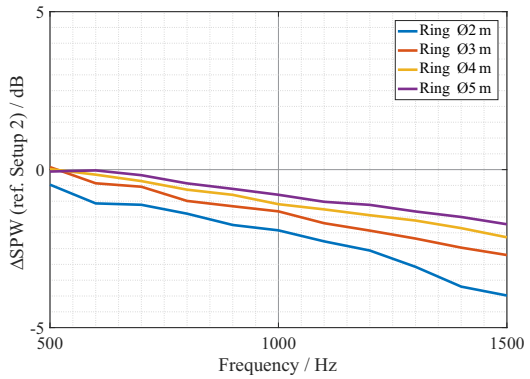


(a)

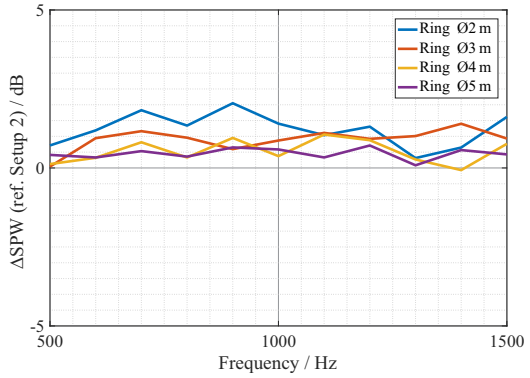


(b)

**Figure 10:** (a) ΔSPW on various ring diameters on SMA/LA8 (b) ΔSPW on various ring diameters on AC8.

If the ring diameter increases, the deviation to the reference, where the tire was omitted, will decrease.

## Conclusion and Outlook

The study showed the influence of a concave curvature on the horn effect. The ΔSPL and ΔSPW were used to quantify the effect. On the largest considered diameter the difference on the sound pressure level was approximately 1.8 dB. Moreover, the influence of a porous and absorbing asphalt was shown. On the absorbing asphalt SMA/LA8 the horn effect was less pronounced. Furthermore, one could see that at larger diameters the deviations become less compared to the situation on a flat road surface. Further investigations will be carried out to see also the effect of a convex curvature. In addition, the position of the acoustic excitation will be varied since previous investigations have shown that the position has an impact on the horn effect.

## References

[1] DIN EN ISO 11819-2, Acoustics-Measurement of the influence of road surfaces on traffic noise-Part2: The close proximity method (2015)

[2] Österreichische Forschungsgesellschafft Straße-Schiene-Verkehr, RVS 11.066 - IV. Rollgeräuschmessung (1997)

[3] AASHTO TP 76-11, Standard Method of Test for Measurement of Tire/Pavement Noise using the On-Board Sound Intensity (OBSI) Method (2013)

[4] Kropp, W. et al.: On the Sound Radiation from Tyres, Acta Acoustica united with Acustica 86 (2000), 769-779

[5] Schutte, J. H. et al., The Influence of the Horn Effect on Tyre/Road Noise, Acta Acoustica united with Acustica 101 (2015), 690-700

[6] Graf, R. A. G. et al.: On the Horn Effect of a Tyre/Road Interface Part I: Experiment and Computation, Journal of Sound an Vibration 256(3) (2002), 417-431

[7] Kaltenbacher, M.: Numerical Simulation of Mechatronic Sensors and Actuators: Finite Elements for Computational Multiphysics, 3rd Edition, Springer, 2015

[8] Schulte, C. et al.: Geräuschminderung von Dünnschichtbelägen, Berichte der Bundesanstalt für Straßenwesen, Heft F 111 (2015)

[9] Wang, H. et al.: Modeling and Optimization of Acoustic Absorption for Porous Asphalt Concrete. Journal of Engineering Mechanics Vol. 142, Issue 4 (April 2016), 2203-2503

[10] DIN EN ISO 10534-2, Acoustics-Determination of sound absorption coefficient and impedance in impedance tubes-Part 2: Transfer function method (2007)